Stochastic FDTD for Analysis of Statistical Variation in Electromagnetic Fields

Steven M. Smith, *Member, IEEE*, and Cynthia Furse, *Fellow, IEEE*

***Abstract*—This paper describes a new stochastic finite difference time domain (S-FDTD) method for calculating the variance in the electromagnetic fields caused by variability or uncertainty in the electrical properties of the materials in the model. Details of the 1D derivation using truncated Taylor series approximations are given. The S-FDTD analysis is then compared to Monte Carlo analysis for a 1D bioelectromagnetic example. The accuracy of the method is controlled by the approximations for the cross correlations of the fields and electrical properties. In this paper, we are able to bound the variance using cross correlations of 1 (overestimate) and the reflection coefficient (underestimate).**

***Index Terms*—Delta method, finite-difference time-domain (FDTD), Monte Carlo, statistics, stochastic FDTD (S-FDTD), variance.**

I. Introduction

THE finite-difference time-domain (FDTD) method is commonly used to evaluate the electromagnetic fields in numerous applications including bioelectromagnetics [1]–[3], geophysical prospecting [4], atmospheric studies [5], [6], etc. As with all electromagnetic simulations, the fields are controlled by the configuration of the model and source, and by the electrical properties of the materials in the model. The particular applications listed here all have one thing in common—their electrical properties vary statistically, either because of variation between individuals, between sections of earth, or between moments of time in the atmosphere. Electrical properties may also have variability because of uncertainty in the measurements, variation in manufacturing, variation in composition, etc. Traditional FDTD simulations use the average values of permittivity and conductivity from these statistically variable materials, and as a result return the average fields produced in that model.

But variation in the model is well known to cause variation in the fields, currents, specific absorption rates (SAR), and other electrical properties of interest. Studies of adults and children using cell phones have shown that size of the head and thickness of the ear have a significant effect on absorbed power [1]–[3]. Other studies [7], [8] have shown the non-negligible effect of head shape. Variability in tissue properties has also been shown to have a significant effect on absorbed power and detuning of implantable antennas [9], [10]. While it is well known that the fields in models with variable properties must also vary statistically, traditional numerical simulations do not provide this information. Estimates have been obtained by running multiple simulations and varying the properties in a variety of ways to determine their effect on output fields. In [1]–[3], [7], [8] a range of models were run with the largest/smallest or highest/lowest values that might be expected. The resultant variation in the fields was found to be significant. But the complexity of the coupling of the electromagnetic fields means that the actual range of fields for an overall population would not necessarily be obtained from any of the example models selected. Useful statistical properties such as variation, standard deviation, 90% confidence intervals, expected maximum or minimum values, etc. cannot be obtained by running selected individual models. A method is needed to determine the variability in electromagnetic fields caused by variability in electrical properties.

The Monte Carlo method [11] is the traditional approach to obtain the statistical variation of the fields from both physical (size) variability and electrical property variability. It was used successfully with 1D FDTD [7] and has also been applied with other numerical methods such as the finite element method (FEM) [12]. Monte Carlo runs a huge number of simulations, selecting the properties for each simulation at 'random' according to their statistics. It produces a collection of the electrical field outputs, which can then be evaluated for their mean and variation. The Monte Carlo method is the 'gold standard' of statistical simulations and produces accurate statistical information on the fields. Unfortunately, it requires thousands or tens of thousands of simulations to complete its analysis, and is therefore too time consuming to be used in many of the real-world simulations that are desired today. The Monte Carlo method will be used to verify the accuracy of the new Stochastic FDTD (S-FDTD) method we describe in this paper using 1D simulations, but it would be impractical to run it for the more complex 3D FDTD simulations used to evaluate cell phone interactions with the human head, for instance.

Perturbation theory [13] is another method that has been used to approximate the impact of small variation in model parameters. In the classical sense it assumes that the solution has a Taylor series expansion which is truncated using only the first few terms. This truncated series is substituted into the equation that is being approximated, and the equation is expanded. The coefficients of the Taylor Series are then determined via linear algebra. This is one of the methods that is used in finding the

Manuscript received September 29, 2011; revised December 21, 2011; accepted January 24, 2012. Date of publication May 01, 2012; date of current version July 02, 2012.

S. Smith is with L3 Communications, Salt Lake City, UT 84116 USA (e-mail: steve.m.smith@comcast.net).

C. Furse is with the Electrical Engineering Department, University of Utah, Salt Lake City, UT 84112 USA (e-mail: cfurse@ece.utah.edu).

Color versions of one or more of the figures in this paper are available online at http://ieeexplore.ieee.org.

Digital Object Identifier 10.1109/TAP.2012.2196962

stochastic properties of mechanical systems using FEM simulations [14]. We will use a Taylor series expansion, i.e., delta method, [26] in the derivation of the S-FDTD method.

This paper addresses the need for a more efficient method of evaluating statistical variation in numerical simulations. It presents a new method to incorporate statistical variation of the electrical properties directly into the traditional FDTD method. Variability in electrical properties causes variability in the electric and magnetic fields, which is carried through the time and space iterations in typical FDTD fashion. This new Stochastic FDTD (S-FDTD) method provides a direct estimate of the mean and variation in the fields at every point in space and time. This paper presents the basic S-FDTD derivation and a discussion of the approximation for cross-correlation that controls its accuracy in Section II, and a 1D bioelectromagnetics example of the feasibility of the method, using a Monte-Carlo simulation to verify its accuracy in Section III. To the best of our knowledge, this is the first simulation of its kind that directly computes the statistical variability of the fields in time and space.

II. Stochastic FDTD (S-FDTD)

Since the finite-difference time-domain method was first conceived by Yee in 1966 [15], numerous adaptations have expanded its functionality. For example, adding the heat equation has enabled calculation of temperature profiles associated with electromagnetic heating [16], [17], adding the plasma fluid equations has enabled analysis of antennas in ionospheric plasma [18], adding Debye or Cole-Cole equations for tissue properties has enabled evaluation of frequency-dependent materials [19]–[22], and near-to-far-field transformations obviate the need to extend the space lattice to the far field [23]. Like these previous adaptations, the S-FDTD method begins with the traditional FDTD approach [15] and adds additional equations to the FDTD iterations to provide additional functionality. In this case, equations for the variance of the electric and magnetic fields are added to enable calculation of their statistics at every point in space and time via the typical FDTD iteration.

Fig. 1 shows the traditional FDTD iteration (shown in white boxes) along with the additions of the variance calculations for the S-FDTD method (shown in grey boxes). The derivations are given in this paper in one dimension (1D) for simplicity and efficiency but are generalizable to 3D as in [24], [25].

The FDTD method [23] (shown here for the TE_z case in 1D) begins with Faraday's law in difference form

$$H_y^{n+1/2}(k+1/2) - H_y^{n-1/2}(k+1/2) = -\frac{\Delta t}{\mu \Delta z}\left(E_x^n(k+1) - E_x^n(k)\right) \quad (1)$$

and Ampere's law in difference form:

$$E_x^{n+1}(k) - \left(\frac{\left(\frac{\varepsilon_r\varepsilon_o}{\Delta t} - \frac{\underline{\sigma}}{2}\right)}{\left(\frac{\varepsilon_r\varepsilon_o}{\Delta t} + \frac{\underline{\sigma}}{2}\right)}\right) E_x^n(k) = -\frac{\left[H_y^{n+1/2}(k+1/2) - H_y^{n+1/2}(k-1/2)\right]}{\left(\frac{\varepsilon_r\varepsilon_o}{\Delta t} + \frac{\underline{\sigma}}{2}\right)\Delta z}. \quad (2)$$

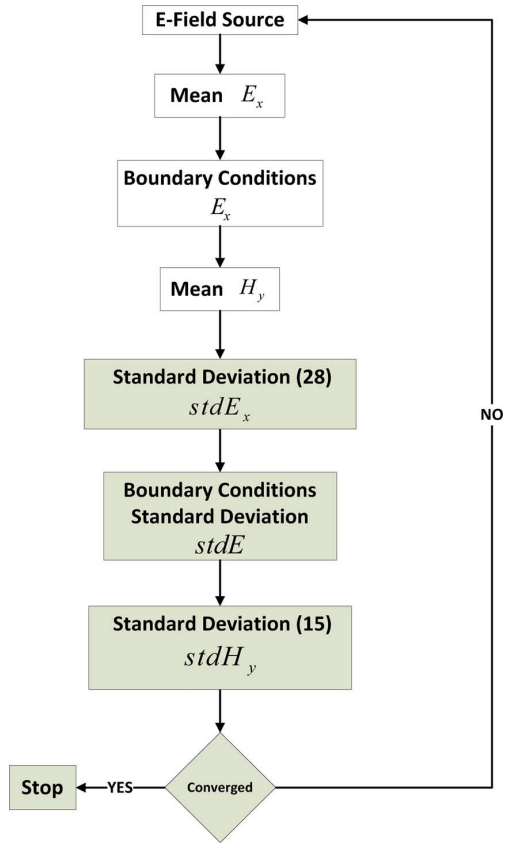

Fig. 1. FDTD (white) and S-FDTD (additions shown in grey) flow chart.

The time index,n, and time step, Δt, control the time resolution of the simulation. The space index,k, and space step, Δz, control the space resolution. They are often related, as they are for the simulations in this paper, by $\Delta t = 2\Delta z/c$, where c is the speed of light. In traditional FDTD simulations the electrical properties, relative permeability, μ_r (=1 for this paper), relative permittivity, ε_r, and conductivity, $\underline{\sigma}$, are taken as the average electrical properties. For the Monte Carlo simulations in Section III, these properties are selected at 'random' based on the statistics for the biological properties in the model. For the S-FDTD method, these properties will have statistical variation, thus altering the equations above. It should be noted that the S-FDTD method can probably be expanded to include variability in the physical size(s) by incorporating variation in the cell sizes Δz within the model, but we have not yet experimented with this aspect of S-FDTD.

A. Mean Field Values

In the S-FDTD derivation, we have stochastic equations (1) and (2) that contain four random variables for the 1D case: E_x, H_y, relative permittivity (ε_r), and the conductivity $(\underline{\sigma})$. The symbol for conductivity has been changed to $(\underline{\sigma})$ to distinguish it from the variance operator σ.

We will use the delta method [26] to derive the mean and variance of the fields in (1) and (2), beginning with the Taylor's series expansion of a generic function, g, of stochastic variables

$x_1, x_2, x_3, \ldots, x_n$. The mean of each of these variables is defined asμ_{x_1}, etc. In our case, the function, g, will be (1) or (2), and the variables will beE_x, H_y, ε_r, or $\underline{\sigma}$

$$g(x_1, x_2, x_3, \ldots, x_n) = g\left(\mu_{x_1}, \mu_{x_2}, \mu_{x_3}, \ldots, \mu_{x_n}\right) + \sum_{i=1}^{n} \left.\frac{\partial g}{\partial x_i}\right|_{\mu_{x_1}, \mu_{x_2}, \ldots, \mu_{x_n}} (x_i - \mu_{x_i}) + \frac{1}{2!}\sum_{i=1}^{n}\sum_{j=1}^{n} \left.\frac{\partial^2 g}{\partial x_i \partial x_j}\right|_{\mu_{x_1}, \mu_{x_2}, \ldots, \mu_{x_n}} (x_i - \mu_{x_i})(x_j - \mu_{x_j}) + \ldots \quad (3)$$

Taking the expectation of (3) and applying the linearity of the expectation operator gives:

$$E\{g(x_1, x_2, x_3, \ldots, x_n)\} = E\left\{g\left(\mu_{x_1}, \mu_{x_2}, \mu_{x_3}, \ldots, \mu_{x_n}\right)\right\} + E\left\{\sum_{i=1}^{n} \left.\frac{\partial g}{\partial x_i}\right|_{\mu_{x_1}, \mu_{x_2}, \ldots, \mu_{x_n}} (x_i - \mu_{x_i})\right\} + E\left\{\frac{1}{2!}\sum_{i=1}^{n}\sum_{j=1}^{n} \left.\frac{\partial^2 g}{\partial x_i \partial x_j}\right|_{\mu_{x_1}, \mu_{x_2}, \ldots, \mu_{x_n}} (x_i - \mu_{x_i})(x_j - \mu_{x_j})\right\} + \ldots \quad (4)$$

Several terms in (4) go to zero. For example, $E\{x_i - \mu_{x_i}\} = E\{x_i\} - \mu_{x_i}$ [27], [28]. Recognizing $E\{x_i\} = \mu_{x_i}$, and the fact that the expectation of a constant is a constant, these terms yield zero. Remembering $E\{aX\} = aE\{X\}$ [27], [28] (4) can now be simplified to:

$$E\{g(x_1, x_2, x_3, \ldots, x_n)\} = g(\mu_{x_1}, \mu_{x_2}, \mu_{x_3}, \ldots, \mu_{x_n}) + \overbrace{\sum_{i=1}^{n} \left.\frac{\partial g}{\partial x_i}\right|_{\mu_{x_1}, \mu_{x_2}, \ldots, \mu_{x_n}} E\{x_i - \mu_{x_i}\}}^{0} + \frac{1}{2!}\sum_{i=1}^{n}\sum_{j=1}^{n} \left.\frac{\partial^2 g}{\partial x_i \partial x_j}\right|_{\mu_{x_1}, \mu_{x_2}, \ldots, \mu_{x_n}} E\{(x_i - \mu_{x_i})(x_j - \mu_{x_j})\} + \ldots \quad (5)$$

Neglecting higher order terms removes the last term of (5), thus showing that:

$$E\{g(x_1, x_2, x_3, \ldots, x_n)\} \approx g\left(\mu_{x_1}, \mu_{x_2}, \mu_{x_3}, \ldots, \mu_{x_n}\right). \quad (6)$$

This is the mathematical verification of the traditional FDTD approach, which says that the average (or expected) fields (the left-hand side of (6)) can be found by solving the field equations using the means or averages of the variables (the right hand side (6)). Thus, the equations for the mean values of the fields in the S-FDTD method are the traditional field (1) and (2). The values E_x and H_y are now recognized to be the mean field values and can be found by inputting the mean electrical properties, ε_r and $\underline{\sigma}$.

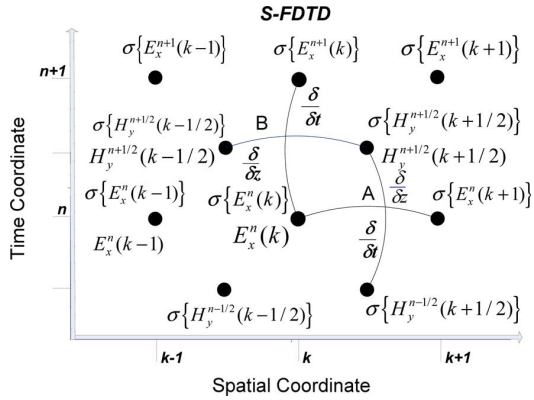

Fig. 2. 1D Yee cell including stochastic variables.

B. Variance of H Fields

We now turn our attention to finding the variance of the fields, which is defined [27], [28]

$$\sigma^2\{g(x_1, x_2, x_3, \ldots, x_n)\} = E\{g(x_1, x_2, x_3, \ldots, x_n)^2\} - E\{g(x_1, x_2, x_3, \ldots, x_n)\}^2 \quad (7)$$

Again using the delta method, expanding (7) in a Taylor's series about the mean of each of the stochastic variables and neglecting the higher order terms gives:

$$\sigma^2\{g(x_1, x_2, x_3, \ldots, x_n)\} = \sum_{i=1}^{n}\sum_{j=1}^{n} \left.\frac{\partial g}{\partial x_i}\frac{\partial g}{\partial x_j}\right|_{\mu_{x_1}, \mu_{x_2}, \ldots, \mu_{x_n}} E\{(x_i - \mu_{x_i})(x_j - \mu_{x_j})\} \quad (8)$$

We will now apply (8) to determine the variance of the fields in (1) and (2). We will also need two identities [27], [28], the variance of the sum of random variables, X and Y:

$$\sigma^2[X \pm Y] = \sigma_X^2 + \sigma_Y^2 \pm 2\mathrm{Cov}(X, Y)$$
$$\sigma^2\{aX\} = a^2\sigma^2\{X\} \quad (9)$$

where a is a constant, and the covariance identity is:

$$\mathrm{Cov}(X, Y) = \rho_{XY}\sigma\{X\}\sigma\{Y\} \quad (10)$$

The two terms in the form of $\sigma\{\cdot\}$ are the standard deviations, and ρ_{XY} is the correlation coefficient.

As with all FDTD equations, it is critical to maintain the correct time and spatial locations for all variables. The Yee cell (Fig. 2) is used in traditional FDTD to identify the locations of the field terms, and the electric and magnetic fields are assumed to be offset by half a time step. We will be adding variables representing the variance of the fields and the electrical properties, so it is important to include them also in the Yee cell (Fig. 2) and associated time representations.

Fig. 2 shows the new 1D S-FDTD cell representation including the new variance variables in space and time. These are the time and space points that will be used in the following derivation of the variances of (1) and (2).

Taking the variance of (1) yields:

$$\sigma^2\left\{H_y^{n+1/2}(k+1/2)-H_y^{n-1/2}(k+1/2)\right\} = \frac{\Delta t^2}{\mu^2\Delta z^2}\sigma^2\left\{E_x^n(k+1)-E_x^n(k)\right\} \quad (11)$$

Applying (9) and rearranging we arrive at:

$$\begin{aligned}&\sigma^2\left\{H_y^{n+1/2}(k+1/2)\right\}+\sigma^2\left\{H_y^{n-1/2}(k+1/2)\right\}\\&-2\rho_{H_{k+1/2}^{n+1/2},H_{k+1/2}^{n-1/2}}\sigma\left\{H_y^{n+1/2}(k+1/2)\right\}\sigma\left\{H_y^{n-1/2}(k+1/2)\right\}\\&=\frac{\Delta t^2}{\mu^2\Delta z^2}\begin{pmatrix}\sigma^2\left\{E_x^n(k+1)\right\}+\sigma^2\left\{E_x^n(k)\right\}\\-2\rho_{E_{k+1}^n,E_k^n}\sigma\left\{E_x^n(k+1)\right\}\sigma\left\{E_x^n(k)\right\}\end{pmatrix}.\end{aligned} \quad (12)$$

Now critical approximations for the correlation coefficients, ρ, must be made. These are bounded between 1 and -1. [27], [28]. The correlation coefficients we are looking for in this case $\rho_{H_{k+1/2}^{n+1/2},H_{k+1/2}^{n-1/2}}$ are between the H fields at time steps $n+1/2$ and $n-1/2$. The two fields are separated by one time stepΔt. These fields are highly correlated to each other, so we can use a correlation coefficient of one [24]. On the right side of (12) we have the correlation coefficient $\rho_{E_{k+1}^n,E_k^n}$ for the two E field terms which are spatially separated from each other by Δz. These are also highly correlated, so we can set the correlation coefficient be equal to one [24].

Using the approximation $\rho = 1$ for these two correlation coefficients and rearranging terms gives:

$$\begin{aligned}&\sigma^2\left\{H_y^{n+1/2}(k+1/2)\right\}\\&-2\sigma\left\{H_y^{n+1/2}(k+1/2)\right\}\sigma\left\{H_y^{n-1/2}(k+1/2)\right\}\\&\qquad+\sigma^2\left\{H_y^{n-1/2}(k+1/2)\right\}\\&=\frac{\Delta t^2}{\mu^2\Delta z^2}\begin{pmatrix}\sigma^2\left\{E_x^n(k+1)\right\}\\-2\sigma\left\{E_x^n(k+1)\right\}\sigma\left\{E_x^n(k)\right\}+\sigma^2\left\{E_x^n(k)\right\}\end{pmatrix}.\end{aligned} \quad (13)$$

This equation has perfectly squared terms on both sides, so we can take the square-root of each side yielding:

$$\left(\sigma\left\{H_y^{n+1/2}(k+1/2)\right\}-\sigma\left\{H_y^{n-1/2}(k+1/2)\right\}\right) = \frac{\Delta t}{\mu\Delta z}\left(\sigma\left\{E_x^n(k+1)\right\}-\sigma\left\{E_x^n(k)\right\}\right). \quad (14)$$

Solving for the variance of the magnetic field yields

$$\sigma\left\{H_y^{n+1/2}(k+1/2)\right\}=\sigma\left\{H_y^{n-1/2}(k+1/2)\right\} +\frac{\Delta t}{\mu\Delta z}\left(\sigma\left\{E_x^n(k+1)\right\}-\sigma\left\{E_x^n(k)\right\}\right). \quad (15)$$

C. Variance of the E Fields

Following the same procedure for the variance of Ampere's law (2) we obtain:

$$\begin{aligned}&\sigma^2\left\{E_x^{n+1}(k)-\frac{\frac{\varepsilon_r\varepsilon_o}{\Delta t}-\frac{\sigma}{2}}{\frac{\varepsilon_r\varepsilon_o}{\Delta t}+\frac{\sigma}{2}}E_x^n(k)\right\}\\&=\sigma^2\left\{\frac{-1}{\left(\frac{\varepsilon_r\varepsilon_o}{\Delta t}+\frac{\sigma}{2}\right)\Delta z}\left(H_y^{n+1/2}(k+1/2)\right.\right.\\&\qquad\left.\left.-H_y^{n+1/2}(k-1/2)\right)\right\}.\end{aligned} \quad (16)$$

Again expanding the left-hand side of (15) using the same identities used for Faraday's Law and setting

$$cc=\frac{\frac{\varepsilon_r\varepsilon_o}{\Delta t}-\frac{\sigma}{2}}{\frac{\varepsilon_r\varepsilon_o}{\Delta t}+\frac{\sigma}{2}} \text{ yields;}$$

$$\begin{aligned}&\sigma^2\left\{E_x^{n+1}(k)-cc\,E_x^n(k)\right\}\\&\quad=\sigma^2\left\{E_x^{n+1}(k)\right\}+\sigma^2\left\{cc\,E_x^n(k)\right\}\\&\qquad-2\mathrm{Cov}\left\{E_x^{n+1}(k),cc\,E_x^n(k)\right\}.\end{aligned} \quad (17)$$

Using the following identity $\mathrm{Cov}(X,Y) = \rho_{X,Y}\sqrt{\sigma^2\{X\}\sigma^2\{Y\}} = \rho_{X,Y}\sigma\{X\}\sigma\{Y\}$ gives:

$$\begin{aligned}&\sigma^2\left\{E_x^{n+1}(k)-cc\,E_x^n(k)\right\}=\sigma^2\left\{E_x^{n+1}(k)\right\}\\&+\sigma^2\left\{cc\,E_x^n(k)\right\}-2\rho_{EE}\sigma\left\{E_x^{n+1}(k)\right\}\sigma\left\{cc\,E_x^n(k)\right\}\end{aligned} \quad (18)$$

with

$$\rho_{EE}=\rho_{E_x^{n+1}(k),cc\,E_x^n(k)}.$$

We will next complete the square of (18). This step of completing the square is very important, because it preserves the phases of the variables. This allows a wave-like function to exist, which in turn allows the use of typical FDTD boundary conditions at the model boundaries. Completing the square of (18), combining terms and simplifying yields:

$$\begin{aligned}&\sigma^2\left\{E_x^{n+1}(k)-cc\,E_x^n(k)\right\}\\&\quad=\left(\sigma\left\{E_x^{n+1}(k)\right\}-\rho_{EE}\sigma\left\{cc\,E_x^n(k)\right\}\right)^2\\&\qquad+\left(1-\rho_{EE}^2\right)\sigma^2\left\{cc\,E_x^n(k)\right\}\end{aligned} \quad (19)$$

Using the same approximation for the squared correlation coefficient ρ_{EE}^2 that was used for Faraday's variance, i.e., E_x fields are highly correlated to each other in time, so we can use a correlation coefficient of one [24] yields the approximation:

$$\begin{aligned}&\sigma^2\left\{E_x^{n+1}(k)-cc\,E_x^n(k)\right\}\\&\qquad\approx\left(\sigma\left\{E_x^{n+1}(k)\right\}-\sigma\left\{cc\,E_x^n(k)\right\}\right)^2\end{aligned} \quad (20)$$

The second term on the right-hand side of (20) is separated using the delta approximation found in (8) thus giving (21), shown at the bottom of the following page.

This equation can now be rearranged in order to complete the square and taking the square-root. Again this preserves the phase of the fields and variance terms. To complete the square of the second term of (21), we would need to have a factor $2\varepsilon_o\mu_{\varepsilon_r}-\Delta t\mu_{\underline{\sigma}}$ to combine with the last term in the equation.

We would also need $(\mu_{\underline{\sigma}}\rho_{\varepsilon_r,E}\sigma\{\varepsilon_r\} - \mu_{\varepsilon_r}\rho_{\underline{\sigma},E}\sigma\{\underline{\sigma}\})^2$. To take the square root of the middle term, we need to remove a -1 from the $-2\varepsilon_o\mu_{\varepsilon_r} + \Delta t\mu_{\underline{\sigma}}$ and change the sign of the second term. To get the third term, we need to add $(\rho_{\varepsilon_r,E}\mu_{\underline{\sigma}}\sigma\{\varepsilon_r\} - \rho_{\underline{\sigma},E}\mu_{\varepsilon_r}\sigma\{\underline{\sigma}\})^2$ and subtract the same from the expression. This is shown in (22) below, which reduces to (23), shown below.

We can now factor out the completed square term and then take the square-root of the equation using the following approximation $\sqrt{1+x} \approx 1 + x/2$ yielding the following:

$$\frac{2\varepsilon_o\mu_{\varepsilon_r} - \Delta t\mu_{\underline{\sigma}}}{2\varepsilon_o\mu_{\varepsilon_r} + \Delta t\mu_{\underline{\sigma}}}\sigma\left\{E_x^n(k)\right\} + \frac{4\Delta t\varepsilon_o\left(\rho_{\varepsilon_r,E}\mu_{\underline{\sigma}}\sigma\{\varepsilon_r\} - \rho_{\underline{\sigma},E}\mu_{\varepsilon_r}\sigma\{\underline{\sigma}\}\right)}{\left(2\varepsilon_o\mu_{\varepsilon_r} + \Delta t\mu_{\underline{\sigma}}\right)^2}E_x^n(k) \quad (24)$$

with a remainder term shown in the last equation at the bottom of the page. Neglecting this remainder we are left with (24) as discussed in [24] resulting in the following approximation:

$$\sigma\left\{\frac{\frac{\varepsilon_r\varepsilon_o}{\Delta t} - \frac{\sigma}{2}}{\frac{\varepsilon_r\varepsilon_o}{\Delta t} + \frac{\sigma}{2}}E_x^n(k)\right\} \approx \frac{2\varepsilon_o\mu_{\varepsilon_r} - \Delta t\mu_{\underline{\sigma}}}{2\varepsilon_o\mu_{\varepsilon_r} + \Delta t\mu_{\underline{\sigma}}}\sigma\left\{E_x^n(k)\right\} + \frac{4\Delta t\varepsilon_o\left(\mu_{\underline{\sigma}}\rho_{\varepsilon_r,E}\sigma\{\varepsilon_r\} - \mu_{\varepsilon_r}\rho_{\underline{\sigma},E}\sigma\{\underline{\sigma}\}\right)}{\left(2\varepsilon_o\mu_{\varepsilon_r} + \Delta t\mu_{\underline{\sigma}}\right)^2}E_x^n(k). \quad (25)$$

Working with the right-hand side of (16) and following the same procedure using the following approximations

$$\rho_{H_{k+1/2}^{n+1/2},H_{k-1/2}^{n+1/2}} \approx 1$$
$$\rho_{\varepsilon_r,H_y^{n+1/2}(k+1/2)} \approx \rho_{\varepsilon_r,H_y^{n+1/2}(k-1/2)}$$
$$\rho_{\sigma,H_y^{n+1/2}(k+1/2)} \approx \rho_{\sigma,H_y^{n+1/2}(k-1/2)}$$

$$\sigma\left\{cc\,E_x^n(k)\right\}^2 \approx \frac{\left(2\varepsilon_o\mu_{\varepsilon_r} - \Delta t\mu_{\underline{\sigma}}\right)^2}{\left(2\varepsilon_o\mu_{\varepsilon_r} + \Delta t\mu_{\underline{\sigma}}\right)^2}\sigma^2\left\{E_x^n(k)\right\} - \frac{8\Delta t\varepsilon_o\left(-2\varepsilon_o\mu_{\varepsilon_r} + \Delta t\mu_{\underline{\sigma}}\right)\left(\rho_{\varepsilon_r,E}\mu_{\underline{\sigma}}\sigma\{\varepsilon_r\} - \rho_{\underline{\sigma},E}\,\mu_{\varepsilon_r}\,\sigma\{\underline{\sigma}\}\right)}{\left(2\varepsilon_o\mu_{\varepsilon_r} + \Delta t\mu_{\underline{\sigma}}\right)^3}\sigma\left\{E_x^n(k)\right\}E_x^n(k) + \frac{16\Delta t^2\varepsilon_o^2\left(-2\rho_{\underline{\sigma},\varepsilon_r}\mu_{\varepsilon_r}\mu_{\underline{\sigma}}\sigma\{\varepsilon_r\}\sigma\{\underline{\sigma}\} + \mu_{\underline{\sigma}}^2\sigma\{\varepsilon_r\}^2 + \mu_{\varepsilon_r}^2\sigma\{\underline{\sigma}\}^2\right)}{\left(2\varepsilon_o\mu_{\varepsilon_r} + \Delta t\mu_{\underline{\sigma}}\right)^4}E_x^n(k)^2 \quad (21)$$

$$\frac{\left(2\varepsilon_o\mu_{\varepsilon_r} - \Delta t\mu_{\underline{\sigma}}\right)^2}{\left(2\varepsilon_o\mu_{\varepsilon_r} + \Delta t\mu_{\underline{\sigma}}\right)^2}\sigma^2\left\{E_x^n(k)\right\} + \frac{8\Delta t\varepsilon_o\left(2\varepsilon_o\mu_{\varepsilon_r} - \Delta t\mu_{\underline{\sigma}}\right)\left(\mu_{\underline{\sigma}}\rho_{\varepsilon_r,E}\sigma\{\varepsilon_r\} - \mu_{\varepsilon_r}\rho_{\underline{\sigma},E}\sigma\{\underline{\sigma}\}\right)}{\left(2\varepsilon_o\mu_{\varepsilon_r} + \Delta t\mu_{\underline{\sigma}}\right)^3}\sigma\left\{E_x^n(k)\right\}E_x^n(k) + \frac{16\Delta t^2\varepsilon_o^2\left(\mu_{\underline{\sigma}}\rho_{\varepsilon_r,E}\sigma\{\varepsilon_r\} - \mu_{\varepsilon_r}\rho_{\underline{\sigma},E}\sigma\{\underline{\sigma}\}\right)^2}{\left(2\varepsilon_o\mu_{\varepsilon_r} + \Delta t\mu_{\underline{\sigma}}\right)^4}E_x^n(k)^2 + \frac{16\Delta t^2\varepsilon_o^2\left(-2\mu_{\varepsilon_r}\mu_{\underline{\sigma}}\rho_{\underline{\sigma},\varepsilon_r}\sigma\{\varepsilon_r\}\sigma\{\underline{\sigma}\} + \mu_{\underline{\sigma}}^2\sigma\{\varepsilon_r\}^2 + \mu_{\varepsilon_r}^2\sigma\{\underline{\sigma}\}^2\right)}{\left(2\varepsilon_o\mu_{\varepsilon_r} + \Delta t\mu_{\underline{\sigma}}\right)^4}E_x^n(k)^2 - \frac{16\Delta t^2\varepsilon_o^2\left(\mu_{\underline{\sigma}}\rho_{\varepsilon_r,E}\sigma\{\varepsilon_r\} - \mu_{\varepsilon_r}\rho_{\underline{\sigma},E}\sigma\{\underline{\sigma}\}\right)^2}{\left(2\varepsilon_o\mu_{\varepsilon_r} + \Delta t\mu_{\underline{\sigma}}\right)^4}E_x^n(k)^2 \quad (22)$$

$$\left\{\frac{2\varepsilon_o\mu_{\varepsilon_r} - \Delta t\mu_{\underline{\sigma}}}{2\varepsilon_o\mu_{\varepsilon_r} + \Delta t\mu_{\underline{\sigma}}}\sigma\left\{E_x^n(k)\right\} + \frac{4\Delta t\varepsilon_o\left(\rho_{\varepsilon_r,E}\mu_{\underline{\sigma}}\sigma\{\varepsilon_r\} - \rho_{\underline{\sigma},E}\mu_{\varepsilon_r}\,\sigma\{\underline{\sigma}\}\right)}{\left(2\varepsilon_o\mu_{\varepsilon_r} + \Delta t\mu_{\underline{\sigma}}\right)^2}E_x^n(k)\right\}^2 + \frac{16\Delta t^2\varepsilon_o^2}{\left(2\varepsilon_o\mu_{\varepsilon_r} + \Delta t\mu_{\underline{\sigma}}\right)^4}E_x^n(k)^2\left(\begin{pmatrix}\mu_{\underline{\sigma}}^2\sigma\{\varepsilon_r\}^2 - 2\rho_{\underline{\sigma},\varepsilon_r}\mu_{\varepsilon_r}\,\mu_{\underline{\sigma}}\,\sigma\{\varepsilon_r\}\sigma\left\{\underline{\sigma}\right\}\\ +\mu_{\varepsilon_r}^2\sigma\{\underline{\sigma}\}^2\end{pmatrix}\right) - \left(\rho_{\varepsilon_r,E}\mu_{\underline{\sigma}}\sigma\{\varepsilon_r\} - \rho_{\underline{\sigma},E}\mu_{\varepsilon_r}\sigma\{\underline{\sigma}\}\right)^2 \quad (23)$$

$$\frac{\frac{16\Delta t^2\varepsilon_o^2}{\left(2\varepsilon_o\mu_{\varepsilon_r}+\Delta t\mu_{\underline{\sigma}}\right)^4}E_x^n(k)^2\begin{pmatrix}\mu_{\underline{\sigma}}^2\left(1-\rho_{\varepsilon_r,E}^2\right)\sigma\{\varepsilon_r\}^2\\ -2\mu_{\varepsilon_r}\mu_{\underline{\sigma}}\left(\rho_{\underline{\sigma},\varepsilon_r} - \rho_{\varepsilon_r,E}\rho_{\sigma,E}\right)\sigma\{\varepsilon_r\}\sigma\left\{\underline{\sigma}\right\}\\ +\mu_{\varepsilon_r}^2\left(1-\rho_{\underline{\sigma},E}^2\right)\sigma\{\underline{\sigma}\}^2\end{pmatrix}}{2\left(\frac{2\varepsilon_o\mu_{\varepsilon_r}-\Delta t\mu_{\underline{\sigma}}}{2\varepsilon_o\mu_{\varepsilon_r}+\Delta t\mu_{\underline{\sigma}}}\sigma\left\{E_x^n(k)\right\} + \frac{4\Delta t\varepsilon_o\left(\mu_{\underline{\sigma}}\rho_{\varepsilon_r,E}\sigma\{\varepsilon_r\} - \mu_{\varepsilon_r}\rho_{\underline{\sigma},E}\sigma\{\underline{\sigma}\}\right)}{\left(2\varepsilon_o\mu_{\varepsilon_r}+\Delta t\mu_{\underline{\sigma}}\right)^2}E_x^n(k)\right)}$$

yields (26), shown at the bottom of the page. Recalling (16) and (20) and taking the square root yields:

$$\sigma\left\{E_x^{n+1}(k)\right\} - \sigma\left\{\frac{\frac{\varepsilon_r\varepsilon_o}{\Delta t} - \frac{\underline{\sigma}}{2}}{\frac{\varepsilon_r\varepsilon_o}{\Delta t} + \frac{\underline{\sigma}}{2}} E_x^n(k)\right\}$$
$$\approx \sigma\left\{\frac{-1}{\left(\frac{\varepsilon_r\varepsilon_o}{\Delta t} + \frac{\underline{\sigma}}{2}\right)\Delta z}\left(H_y^{n+1/2}(k+1/2) - H_y^{n+1/2}(k-1/2)\right)\right\}.$$

Substituting (25) and (26) yields (27) and solving for $\sigma\{E_x^{n+1}(k)\}$

$$\begin{aligned}\sigma\left\{E_x^{n+1}(k)\right\} \approx{}& \frac{2\varepsilon_o\mu_{\varepsilon_r} - \Delta t\mu_{\underline{\sigma}}}{2\varepsilon_o\mu_{\varepsilon_r} + \Delta t\mu_{\underline{\sigma}}}\sigma\left\{E_x^n(k)\right\} \\ &+ \frac{2\Delta t}{\Delta z(2\varepsilon_o\mu_{\varepsilon_r} + \Delta t\mu_{\underline{\sigma}})}\begin{pmatrix}\sigma\left\{H_y^{n+1/2}(k+1/2)\right\} \\ -\sigma\left\{H_y^{n+1/2}(k-1/2)\right\}\end{pmatrix} \\ &+ \frac{4\Delta t\varepsilon_o\left(\mu_{\underline{\sigma}}\rho_{\varepsilon_r,E}\sigma\{\varepsilon_r\} - \mu_{\varepsilon_r}\rho_{\underline{\sigma},E}\sigma\{\underline{\sigma}\}\right)}{\left(2\varepsilon_o\mu_{\varepsilon_r} + \Delta t\mu_{\underline{\sigma}}\right)^2}E_x^n(k) \\ &- \frac{2\Delta t}{\Delta z(2\varepsilon_o\mu_{\varepsilon_r} + \Delta t\mu_{\underline{\sigma}})} \\ &\times\begin{pmatrix}\frac{\left(2\varepsilon_o\sigma\{\varepsilon_r\}\rho_{\varepsilon_r,H_y^{n+1/2}} + \Delta t\sigma\{\underline{\sigma}\}\rho_{\underline{\sigma},H_y^{n+1/2}}\right)}{\left(2\varepsilon_o\mu_{\varepsilon_r} + \Delta t\mu_{\underline{\sigma}}\right)} \\ \times\left(H_y^{n+1/2}(k-1/2) - H_y^{n+1/2}(k+1/2)\right)\end{pmatrix}. \quad (27)\end{aligned}$$

Equations (15) and (27) are new equations for the variance of the magnetic and electric fields, respectively. They require approximations for the correlation coefficients ρ, which we will bound in the example in Section III. Correlation coefficients are bounded between 1 and -1 [28]. We tried a number of different approximations for the correlation coefficients, and have shown bounding results from two of them in Section III. Using a correlation coefficient of 1 was found to overestimate the variance. Another option is to use a correlation related to the reflection coefficient from the nearest boundary in the 1D layered model. This was found to underestimate the variance. Monte Carlo analysis could be used to exactly predict the correlation coefficients, but of course by the time you were finished with the Monte Carlo, there would be no need to run an S-FDTD simulation. The approximation for correlation coefficients is an area warranting further research in this method, but for now we will proceed using either the high value of 1 or the low value of the reflection coefficient of the nearest boundary (explained in more detail in Section III), and proceed.

Interestingly, the variances of the fields behave much like waves. They are incorporated into the FDTD iteration as shown in Fig. 1, where the variance of each field is computed after the mean value of the field. The mean values of the fields are computed using the traditional FDTD (1) and (2). Both the mean field values and their variances behave like waves, and thus require a boundary condition (28) on one of the waves. This is also shown in the flow chart in Fig. 1.

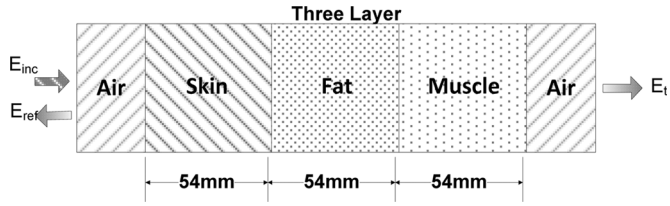

Fig. 3. 1D Layered tissue model.

$$E_x^{n+1}(0) = E_x^n(1) + \frac{c\Delta t - \Delta x}{c\Delta t + \Delta x}\left[E_x^{n+1}(1) - E_x^n(0)\right]$$

and

$$\begin{aligned}E_x^{n+1}(N\Delta x) = E_x^n(N\Delta x) &+ \frac{c\Delta t - \Delta x}{c\Delta t + \Delta x}\left[E_x^{n+1}((N-1)\Delta x)\right. \\ &\left. - E_x^n(N\Delta x)\right] \quad (28)\end{aligned}$$

with the boundaries occurring at 0 and $N\Delta x$.

The variance acts like another wave, which reflects off the boundary if not terminated. Standard boundary conditions can be used to prevent this reflection at model space boundaries.

III. Layered Tissue Example

In order to evaluate the accuracy of the S-FDTD method, a 1D layered tissue model shown in Fig. 3 was evaluated with both Monte Carlo and S-FDTD. The relative permittivity (ε_r) and conductivity $(\underline{\sigma})$ of each layer have statistical variations given in Table I.

A 2 GHz plane wave impinging from the left was used as the source. The spatial step was set to the largest wavelength within the model space divided by 40 and the time step was set equal to the spatial step divided by $2c_o$.

Monte Carlo analysis was used to determine the exact mean and variance of the fields in this model. 10 000 FDTD simulations were done, after which the mean and variance of the fields

$$\sigma\left\{\frac{-1}{\left(\frac{\varepsilon_r\varepsilon_o}{\Delta t} + \frac{\underline{\sigma}}{2}\right)\Delta z}\left(H_y^{n+1/2}(k+1/2) - H_y^{n+1/2}(k+1/2)\right)\right\}$$
$$\approx \frac{2\Delta t}{\Delta z(2\varepsilon_o\mu_{\varepsilon_r} + \Delta t\mu_{\underline{\sigma}})}\begin{pmatrix}\sigma\left\{H_y^{n+1/2}(k+1/2)\right\} - \sigma\left\{H_y^{n+1/2}(k-1/2)\right\} \\ -\frac{\left(2\varepsilon_o\sigma\{\varepsilon_r\}\rho_{\varepsilon_r,H_y^{n+1/2}} + \Delta t\sigma\{\underline{\sigma}\}\rho_{\underline{\sigma},H_y^{n+1/2}}\right)}{\left(2\varepsilon_o\mu_{\varepsilon_r} + \Delta t\mu_{\underline{\sigma}}\right)} \\ \cdot\left(H_y^{n+1/2}(k-1/2) - H_y^{n+1/2}(k+1/2)\right)\end{pmatrix} \quad (26)$$

TABLE I
MATERIAL PROPERTIES [29]

Dielectric	ε_r Mean	ε_r [SD]	$\underline{\sigma}$ Mean (S/m)	$\underline{\sigma}$ [SD]	Thickness (mm) d_i
Muscle	55.0	4.6	0.87	0.10	42
Fat (infiltrated)	16.2	2.7	0.214	0.06	54
Skin	39.0	3.4	0.43	0.10	5.4

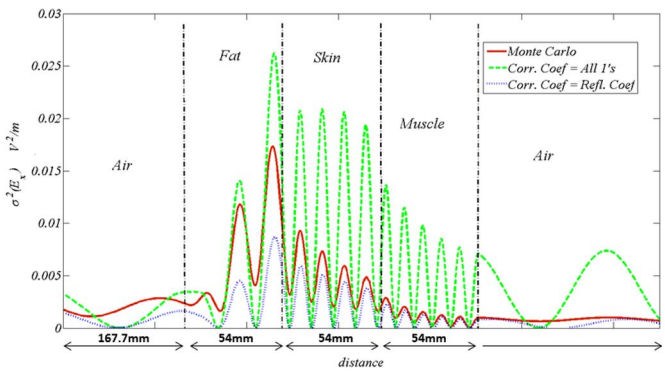

Fig. 4. Three Layer 2 GHz E field Variance.

were computed from their outputs. The input electrical properties for each simulation were chosen assuming that the permittivity and conductivity were normally distributed with the parameters given in Table I.

For all cases, the mean of the S-FDTD method (which is equivalent to the traditional FDTD method) was within approximately .02 V/m of the Monte Carlo mean values with a 1 V/m plane wave. This verifies that the approximation in (6) is accurate for this application.

The variance of the electric field is shown in Fig. 4. The Monte Carlo results are assumed to be the most accurate. The S-FDTD variances using the correlation coefficients of 1 overestimate this variance and the correlation coefficients equal to the reflection coefficients, taken at dielectric boundaries and used throughout the dielectric material, slightly underestimate the variance. This characteristic was seen in numerous similar examples, only one of which is shown here. Although still not exact, we are encouraged that we are able to bound the Monte Carlo-computed variances using two simple S-FDTD runs, and that each of these approximations evaluate the variance at least to within an order of magnitude. More research on a better approximation for the correlation coefficient would be expected to tighten up the accuracy of these results.

IV. CONCLUSION

This paper describes a new Stochastic FDTD (S-FDTD) method that provides a more efficient method of evaluating statistical variation in numerical simulations. Statistical variation of the electrical properties is incorporated directly into the traditional FDTD method. Variation of the electric and magnetic fields in both space and time is computed directly in the FDTD iteration. This new Stochastic FDTD (S-FDTD) method provides a direct estimate of the mean and variation in the fields at every point in space and time.

As an example of this method, we computed the variance of the fields in a simple 1D bioelectromagnetics example (layered skin-fat-muscle). Field variances computed using S-FDTD were compared to those computed using Monte-Carlo, and good agreement was found, validating the method. The accuracy of this method is controlled by the approximations for cross correlations of the fields and electrical properties of the materials. In this paper, we have bounded the variance of the fields by using a cross correlation of 1 (overestimate) and a reflection coefficient (underestimate). Additional future research is warranted to improve this estimate. This method is not limited to 1D. It has been extended to 3D in [24].

The total additional memory for the S-FDTD method is double that for the traditional FDTD method, since now we must store the variance of the fields in addition to the fields themselves. The simulation time is also slightly more than doubled, as now we have twice as many equations to compute. The variance equation for Ampere's law (27) is somewhat more complicated than the other equations, thus requiring additional computational time. Still, when compared with having to run hundreds, thousands, or more of Monte Carlo simulations, the S-FDTD method offers a huge savings in computation time. This new method provides a way to compute the variance in the fields caused by variance in the electrical properties in the model. This opens up the possibility of additional assessment of confidence intervals, expected variation, and other statistical parameters for applications such as bioelectromagnetics, geophysical prospecting, and studies of ionospheric plasma where the electrical properties have uncertainty or variability.

ACKNOWLEDGMENT

We would like to thank Dr. C. Gabriel for providing the electrical properties of human tissues used in the simulations.

REFERENCES

[1] O. P. Gandhi, G. Lazzi, and C. Furse, "Electromagnetic absorption in the human head and neck for mobile telephones at 835 and 1900 MHz," *IEEE Trans. Microwave Theory Tech.*, vol. 44, pp. 1884–1897, Oct. 1996, 1996.

[2] C. M. Furse, G. Lazzi, and O. P. Gandhi, "FDTD computation of power deposition in the head for cellular telephones," in *Antennas and Propagation Society Int. Symp. AP-S. Digest*, 1996, vol. 3, pp. 1794–1797.

[3] V. Pandit, R. McDermott, G. Lazzi, C. Furse, and O. Gandhi, "Electrical energy absorption in the human head from a cellular telephone," in *Proc. Visualization'96*, 1996, pp. 371–374.

[4] D. Johnson, E. Cherkaev, C. Furse, and A. Tripp, "Cross-borehole delineation of a conductive ore deposit—Experimental design," *Geophysics*, pp. 824–835, May/Jun. 2001.

[5] J. Ward, C. Swenson, and C. Furse, "The impedance of a short dipole antenna in a magnetized plasma via a FDTD model," *IEEE Trans. Antennas Propag.*, vol. 53, pp. 2711–2718, Aug. 2005.

[6] J. J. Simpson and A. Taflove, "A review of progress in FDTD Maxwell's equations modeling of impulsive subionospheric propagation below 300 kHz," *IEEE Trans. Antennas Propag.*, vol. 55, pp. 1582–1590, Jun. 2007.

[7] A. Christ and N. Kuster, "Differences in RF energy absorption in the heads of adults and children," *Bioelectromagnetics*, pp. S31–S44, 2005.

[8] B. B. Beard, W. Kainz, T. Onishi, T. Iyama, S. Watanabe, O. Fujiwara, W. Jianqing, G. Bit-Babik, A. Faraone, J. Wiart, A. Christ, N. Kuster, L. Ae-Kyoung, H. Kroeze, M. Siegbahn, J. Keshvari, H. Abrishamkar, W. Simon, D. Manteuffel, and N. Nikoloski, "Comparisons of computed mobile phone induced SAR in the SAM phantom to that in anatomically correct models of the human head," *IEEE Trans. Electromagn. Compat.*, vol. 48, pp. 397–407, 2006.
[9] J. D. Johnson, "Statistical Analysis of Detuning Effects for Implantable Microstrip Antennas," Masters of Science thesis, Elect. Comput. Engrg. Dept., Univ. Utah, Salt Lake City, 2007.
[10] J. D. Johnson and C. Furse, "Statistical analysis of detuning effects for implantable microstrip antennas," presented at the North American Radio Science Conference URSI-CNC/USNC, Ottawa, Canada.
[11] M. N. O. Sadiku, *Numerical Techniques in Electromagnetics*, 2nd ed. Boca Raton, FL: CRC Press, 2001.
[12] L. Fang, Q. H. Cen, K. Sun, W. M. Liu, X. F. Zhang, and Z. F. Huang, "FEM computation of groove ridge and Monte Carlo simulation in two-body abrasive wear," *Wear*, vol. 258, pp. 265–274, Jan. 2005.
[13] A. Nayfeh, *Perturbation Methods*, 1st ed. New York: Wiley, 1973.
[14] M. Kleiber and T. D. Hein, *The Stochastic Finite Element Method Basic Perturbation Technique and Computer Implementation*, 1st ed. New York: Wiley, 1992.
[15] Y. Kane, "Numerical solution of initial boundary value problems involving Maxwell's equations in isotropic media," *IEEE Trans. Antennas Propag.*, vol. 14, pp. 302–307, 1966.
[16] A. S. Nagra and R. A. York, "FDTD analysis of wave propagation in nonlinear absorbing and gain media," *IEEE Trans. Antennas Propag.*, vol. 46, pp. 334–340, 1998.
[17] P. C. Cherry and M. F. Iskander, "FDTD analysis of power deposition patterns of an array of interstitial antennas for use in microwave hyperthermia," *IEEE Trans. Microwave Theory Tech.*, vol. 40, pp. 1692–1700, 1992.
[18] J. Ward, C. Swenson, and C. Furse, "The impedance of a short dipole antenna in a magnetized plasma via a FDTD model," *IEEE Trans. Antennas Propag.*, vol. 53, pp. 2711–2718, Aug. 2005, 2005.
[19] R. M. Joseph, S. C. Hagness, and A. Taflove, "Direct time integration of Maxwell's equations in linear dispersive media with absorption for scattering and propagation of femtosecond electromagnetic pulses," *Opt. Lett.*, vol. 16, pp. 1412–1414, 1991.
[20] R. Luebbers, F. P. Hunsberger, K. S. Kunz, R. B. Standler, and M. Schneider, "A frequency-dependent finite-difference time-domain formulation for dispersive materials," *IEEE Trans. Electromagn. Compat.*, vol. 32, pp. 222–227, 1990.
[21] D. M. Sullivan, "A frequency-dependent FDTD method for biological applications," *IEEE Trans. Microwave Theory Tech.*, vol. 40, pp. 532–539, 1992.
[22] O. P. Gandhi, B. Q. Gao, and J. Y. Chen, "A frequency-dependent finite-difference time-domain formulation for general dispersive media," *IEEE Trans. Microwave Theory Tech.*, vol. 41, pp. 658–665, 1993.
[23] A. Taflove and S. C. Hagness, *Computational Electrodynamics the Finite Time-Difference Domain Method*, 3rd ed. Norwood, MA: Artech House, 2005.
[24] S. M. Smith and C. Furse, "Stochastic FDTD," Ph.D. dissertation, Univ. Utah, Salt Lake City, UT, 2011.
[25] S. M. Smith and C. Furse, "A stochastic FDTD method for statistically varying biological tissues," presented at the 2 IEEE AP-S Int. Symp. on Antennas and Propagation and USNC/CNC/URSI, Spokane, WA, 2011.
[26] R. L. B. G. Casella, *Statistical Inference*, 2nd ed. Pacific Grove: Duxbury, Thompson Learning, 2002.
[27] V. Krishnan, *Probability and Random Process*, 1st ed. Hoboken, NJ: Wiley, 2006.
[28] R. H. M. Ronald, E. Walpole, S. L. Myers, and K. Ye, *Probability and Statistics for Engineers and Scientists*. Upper Saddle River, NJ: Pearson Prentice-Hall, 2007, p. 816.
[29] C. Gabriel, "Personal communication," 2006.

Steven M. Smith (M'11) received the B.S.E.E. degree in 1985, the M.S.E.E. degree in 2007, and the Ph.D. degree in 2011 all from the University of Utah, Salt Lake City.

He is a Senior Staff Engineer with L-3 Communications, Salt Lake City, and an Adjunct Assistant Professor at the University of Utah, Salt Lake City.

His expertise is in RF and microwave circuit design, he has worked in land mobile radio industry and currently designs transceiver circuits for high speed modems. He has also taught Microwave Engineering II in active circuit design. His research interests in include microwave circuit design and simulation.

Cynthia M. Furse (F'08) received the B.S.E.E. degree in 1985, the M.S.E.E. degree in 1988, and the Ph.D. EE degree in 1994 all from the University of Utah, Salt Lake City.

Currently, she is the Associate Vice President for Research at the University of Utah, Salt Lake City, and a Professor in the Electrical and Computer Engineering Department. Her expertise in electromagnetics is applied to sensing and communication in complex lossy scattering media such as the human body, geophysical prospecting, ionospheric plasma, and aircraft wiring networks. She has taught electromagnetics, wireless communication, computational electromagnetics, microwave engineering, and antenna design. She works to interest young students in engineering and routinely volunteers in Utah's K-12 schools.

Dr. Furse is a Fellow of the IEEE. She received the Harriett B. Rigas award for educational excellence from the IEEE in 2009. She is active with the Society of Women Engineers, Expanding your Horizons, School-to-Careers, MESA, Girl Scouts and Boy Scouts.